Journal of ELECTRICAL ENGINEERING, VOL. 54, NO. 1-2, 2003, 42–46

COMMUNICATIONS

WAVELET PACKET TRANSFORM IN RAW ULTRASOUND SIGNAL PROCESSING

Radim Kolář — Jiří Kozumplík *

A new modification of incoherent processing (IP) method for speckle reduction in ultrasound (US) images has been developed. This method combines filtering of the radiofrequency (RF) signal with the wavelet packet filters and envelope averaging to enhance classical incoherent methods. The comparison with standard IP method is made.

K e y w o r d s: wavelet transform, ultrasound imaging, radiofrequency signal, incoherent processing

1 INTRODUCTION

The speckles and poor contrast of ultrasound images affect human interpretation and make the image analysis unreliable. Speckles arise from the interferences of the acoustic pulses within the resolution cell and are therefore correlated with the object roughness.

A number of approaches for speckle reduction in B-mode images have been published in last twenty years. These include geometric filtering [1],Wiener filtering [2], adaptive methods [3, 4], and the methods based on the discrete wavelet transform (DWT) [5, 6, 7] in 2D images. In radiofrequency (RF) domain little work has been done, *eg* IP [8, 9]. In this paper, we present a connection between the IP method with the wavelet packet (WP) filters to reduce the speckles level in B-mode images.

2 METHOD

2.1 Incoherent processing

The IP method (Fig. 1), also called frequency compounding, frequency-diversity, or split spectrum processing, is a method for speckle reduction, which utilizes the RF signal [8, 9]. The ultrasound image consists of columns (RF signals) which create the B-scan. Therefore the processing is performed in 1D. Each RF signal is first processed with narrowband filters spanning the bandwidth of the ultrasound probe. The signals from these filters are envelope detected to create narrowband images. These images are usually normalized to equalize their amplitude and summed. As the speckles from various frequency bands are rather decorrelated, speckle reduction is achieved. The properties of the filters (the bandwidth and central frequency) depend on the properties of the ultrasound probe and desired speckle reduction.

The main disadvantage of this method is that there is a trade off between the level of speckles reduction and the axial resolution. The narrower the filters bandwidth, the higher the speckles suppression and the worse the axial resolution. This blurring could cause a loss of some details. For maximal speckles suppression the narrowband images have to be uncorrelated. This can be achieved when the bandpass filters are orthogonal - correlation between their frequency responses is zero. From decorrelation point of view the wavelet filters are more convenient than other filters.

2.2 Wavelet packet transform

The DWT has found many applications in signal and image processing. It decomposes the signal into several levels with different scales by filter banks. Although the dyadic decomposition is used very often, we have used the packet DWT without decimation, which is more convenient for our application.

The WP decomposition scheme without decimation is shown in Fig. 2. The input signal is filtered by the high-pass filter $G(z)$ to achieve the signal representing high-frequency components and by lowpass filter $H(z)$ representing low-frequency components. Therefore we split the input signal into two subbands, which are decomposed further by bandpass filters, that arise from $G(z)$ and $H(z)$. The main difference between the dyadic and packet decomposition is that in the dyadic case we decompose only the low-frequency from the previous level. Therefore, the WP offers richer signal analysis.

* Department of Biomedical Engineering, Faculty of Electrical Engineering and Communication, Brno University of Technology, Purkyňova 118, 612 00 BRNO, Czech Republic, e-mail: kolarr@feec.vutbr.cz

ISSN 1335-3632

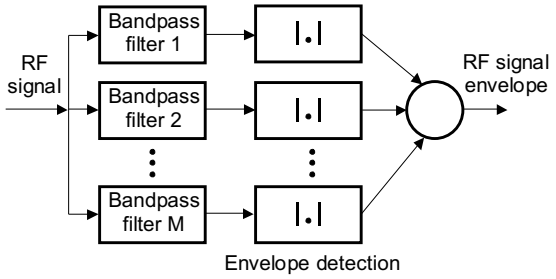

Fig. 1. The basic schema of incoherent processing method

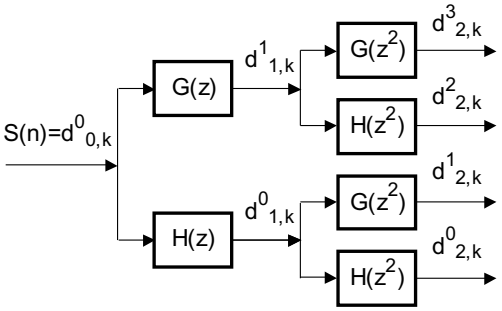

Fig. 2. The packet decomposition scheme for level $J = 2$.

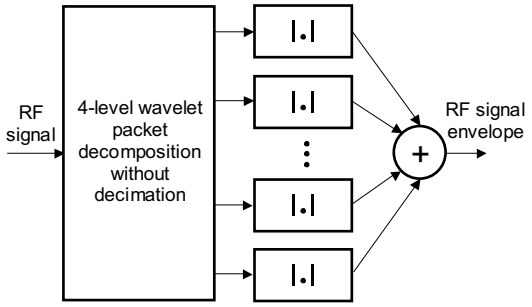

Fig. 3. The schema of IP method with PD.

The WP decomposition without decimation can be performed by convolution [10]:

$$\begin{aligned} d_{j,k}^{2p} &= \sum_{m=-\infty}^{+\infty} d_{j-1,m}^{p}\big(h_j(k-m)\big) \\ d_{j,k}^{2p+1} &= \sum_{m=-\infty}^{+\infty} d_{j-1,m}^{p}\big(g_j(k-m)\big), \end{aligned} \tag{1}$$

where $h_j(k)$ or $g_j(k)$ arises from the impulse responses of $G(z)$ or $H(z)$ filters by inserting $j-1$ zeros between the samples as indicated in Fig. 2 by z^j.

In the case of full WP decomposition the frequency plane is divided into the 2^J equidistant subbands, where J is the decomposition level. It should be mentioned that this decomposition has not to be full. This means that we can decompose the signal according to the frequency content of the input signal.

2.3 Connection between IP and WP

Based on the previous paragraphs, we are now ready to formulate our approach. This method utilizes the wavelet packet decomposition for each RF signal creating the image. Therefore only 1D implementation is needed. After decomposition, the signals from each subband are envelope detected and summed to reduce the speckles. The scheme of this method is depicted in Fig. 3.

The choice of the level decomposition J is connected with the frequency properties of the RF signal and with the desirable speckle suppression. In our case, the frequency of RF signal is ranging from 0.5 MHz to 5 MHz. The sampling frequency was 20 MHz. Therefore the $J = 4$ appears as a reasonable choice between the speckle suppression and loss of axial resolution. For this level the frequency plane was divided into 16 subbands with 625 kHz width. However, only 8 subbands that lie in a range from 0 to 5 MHz are usable. Therefore we did not need to perform full WP decomposition. This also speeds up the computation.

The choice of the wavelet filters is another problem that has to be solved. We used the Daubechies wavelet filters (abbreviated as $db1$, $db2$, ... according to order) because of their orthogonality and their maximally flat frequency responses [10]. Below we will show the influence of the filter's order on the resultant B-mode image.

3 EXPERIMENTAL RESULTS AND DISCUSSION

A tissue mimicking phantom (RMI 403GS) and tissue of the pig heart were used for the tests. Each image frame consisted of 78 A-scans which were separately processed by the proposed modified IP method. After processing, the B-mode image was created by linear interpolation and logarithmic amplitude compression.

For comparison, the IP with *non-wavelet* filters were used. These filters have magnitude frequency responses described as [9]

$$H(f) = \cos^2\left[\frac{\pi(f-f_c)}{10^6}\right], \tag{2}$$

where f_c is the position of maxima and it holds $-500\,\text{kHz} \le f - f_c \le 500\,\text{kHz}$. 8 filters were used in the range from 0.625 MHz to 5.2 MHz.

The "quality" of an object (*eg* lesion) is usually measured by contrast-to-noise ratio (CNR), which can be defined as [9]:

$$CNR = \frac{\mu_o - \mu_b}{\sqrt{\sigma_o^2 + \sigma_b^2}} \tag{3}$$

where μ_o and μ_b are the mean values of the object and background, respectively. σ_o and σ_b correspond to the standard deviations of the object and background. The

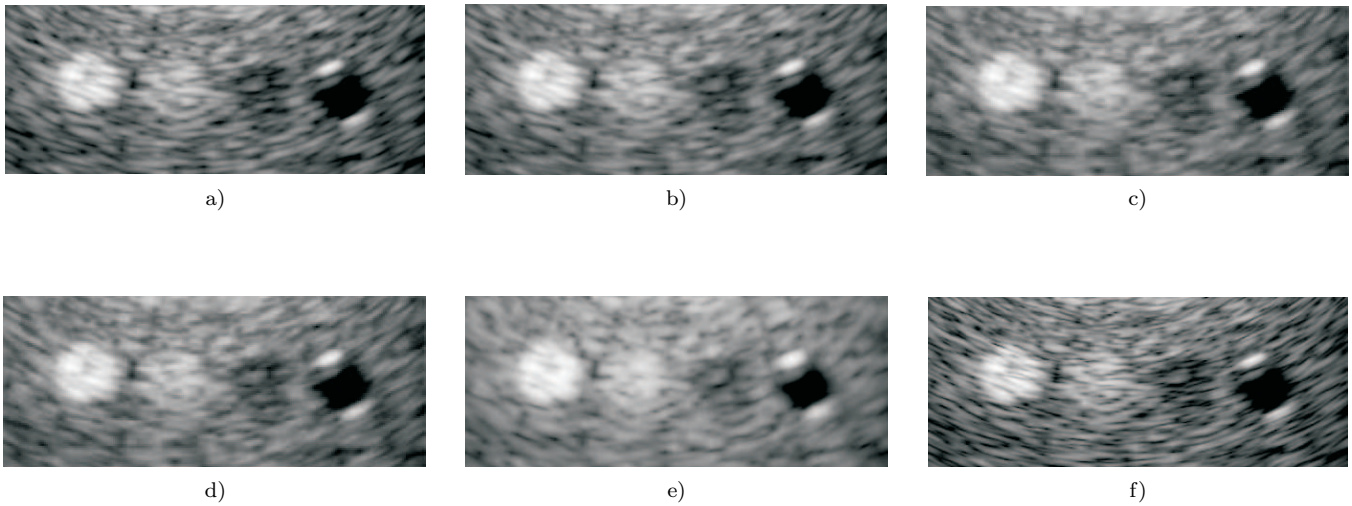

Fig. 4. Four objects $(1, 2, 3, 4$ from left to right)in phantom image processed by IP method with WP decomposition: a) *db1*, b) *db2*, c) *db3*, d) *db4*, e) standard IP method, f) original

Table 1. The CNR and SI Values for Phantom Image

	CNR				**SI**			
object	**1**	**2**	**3**	**4**	**1**	**2**	**3**	**4**
db1	8.92	8.64	4.70	1.55	2.89	1.80	1.26	3.59
db2	9.96	9.54	5.18	1.54	3.11	1.91	1.34	3.84
db3	10.80	7.93	5.66	1.60	3.25	2.03	1.41	4.02
db4	10.82	11.70	6.10	1.61	3.24	2.11	1.47	4.07
db5	10.31	11.59	6.60	1.51	3.12	2.02	1.51	3.79
IP	13.66	12.85	7.14	1.98	3.39	2.15	1.47	3.70
original	7.48	6.30	3.59	1.53	2.44	1.42	1.05	3.13

speckles can be quantified by the means of speckle index (SI) evaluated for homogeneous region [1]:

$$SI = \frac{\mu}{\sigma} \tag{4}$$

where μ and σ are the region mean value and standard deviation. Table 1 shows the CNR and SI values for the four phantom objects (see Fig. 4). The region for CNR evaluation were marked manually inside and outside the objects. The SI values were calculated only inside of these regions. When comparing these values, the processed images should be taken into account in order to compare the axial resolution visually. We can see that the standard IP method has higher values of SI and CNR, but the smoothing and the loss of axial resolution is quite high. This can be seen from Fig. 4f, especially from the object on the right, because the reflections on its borders are appreciably blurred. The images obtained by IP method with WP decomposition show various level of this blurring depending on the order of Daubechies filters.

Based on the quantitative results in Table 1 and qualitative results from the images, the Daubechies wavelet filters of order 3 and 4 appear to be appropriate for our purpose. For the higher order filter the image smoothing is too high and also the improvement of CNR and SI is not significantly higher.

Figure 5 shows the original image of the *in vivo* pig heart (a) and the same image obtained by the IP method with WP decomposition (b) with Daubechies filters of order 3 and by standard IP method (c). We can see that the image after processing by IP packet contains a lower level of speckles and also the object borders are "more continuous". Therefore, the processed images are more convenient for prospective edge detection or object delineation. The image after standard IP method shows also a certain level of speckle elimination, but on the other hand the level of blurring is quite high. This could cause a loss of some detail structures.

To compare the axial resolution we can study a line profile in B-mode image that contains objects that should stay separated after processing. The position of the line profile is indicated in Fig. 5a. The corresponding 1D line profiles are shown in Fig. 6. The markers 1 and 2 indicate the mitral valve that exhibits itself as bright stripes. These stripes should stay separated after processing. The markers 3 and 4 indicate the cardiac muscle, where speckles are present, and after processing it should be "smoother".

Figure 6a shows the original profile (thin line) and the profile after processing by standard IP method (bold line). We can see that after processing the two sharp spikes were smoothed and they became one spike. Figure 6b shows the result after IP with WP decomposition with *db*3 filters. Although the spikes 1 and 2 are decreased in comparison with the original, they almost stay separated and sharp. Also the speckles between points 3 and 4 are reduced.

4 CONCLUSION

A new modified IP method has been presented. The wavelet packet filters seem to be a good alternative to

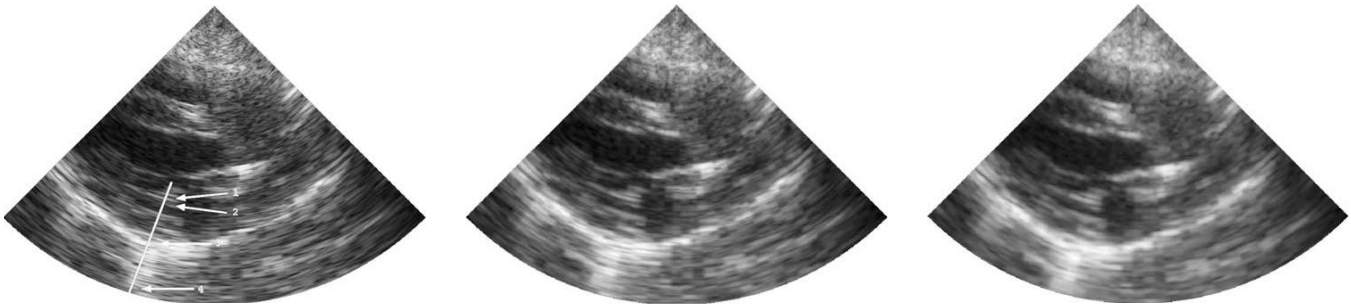

a) b) c)

Fig. 5. B-mode images of the pig heart. a) the original image, b) image obtained by IP method with WP decomposition with *db3* filters, c) image after standard IP method.

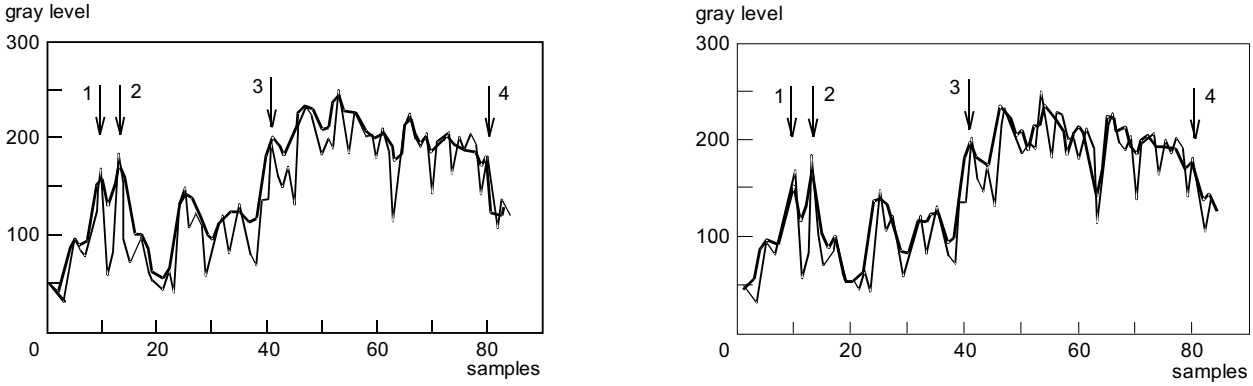

a) b)

Fig. 6. The line profile after a) standard IP and b) IP with WP decomposition. Thin line indicates original profile and bold line, the profile after processing. See text for details.

current filters, because of their orthogonality. It has been shown that the type of wavelet filters has a significant influence on the axial resolution, CNR and SI values. Beside this parameter, the speckle reduction can also be controlled by the decomposition level, which depends especially on the frequency content of the RF signal. In comparison with the standard IP, the IP with WP decomposition offers the freedom to chose from various kind of filters that maintain orthogonality.

In this study we have focused only on the basic form of the IP method, but this method offers more possibilities. For example utilizing only particular frequency bands, where some pathological changes in the tissue show some variations, *etc*. This will need more research.

Acknowledgments

This work has been supported by the grant No. 102/02/0890 of the Grant Agency of the Czech Republic, grant project B2813303 of the Czech Academy of Science and the Research Programme of Brno University of Technology CEZ J22/98:262200011.

The authors wish to thank to Laboratory for Medical Imaging Research at Katholieke Universiteit Leuven in Belgium for performing the ultrasonic measurement.

References

[1] CRIMMINS, T.R.: Geometric Filter for Speckle Reduction, Applied Optics **24** No. 10 (1985), 1438–1443.

[2] JAN, J.—KILIAN, P.: Modified Wiener Approach to Restoration of Ultrasonic Scans via Frequency Domain, in Proc. The 9th Scandinavian Conference on Image Analysis, 1995, pp. 1173–1180.

[3] DUTT, V.—GREENLEAF, J.F.: Adaptive Speckle Reduction Filter for Log-Compressed B-Scan Images, IEEE Transaction on Medical Imaging **15** No. 6 (1996), 802–813.

[4] KARAMAN, M.—KUTAY, M.A.—BOZDAGI, G.: An Adaptive Speckle Supression Filter for Medical Ultrasonic Imaging, IEEE Transaction on Medical Imaging **14** No. 2 (1995), 283–292.

[5] GAGNON, L.—JOUAN, A.: Speckle Filtering of SAR Images — A Comparative Study Between Complex-Wavelet-Based and Standard Filters, Wavelet Applications in Signal and Image Processing, San Diego, 1997, pp. 80–91.

[6] HAO, X.—GAO, S.—GAO, X.: A Novel Multiscale Nonlinear Thresholding Method for Ultrasonic Speckle Suppressing, IEEE Transactions on Medical Imaging **18** No. 9 787–794 (1999).

[7] XULI ZONG-LAINE, A.F.—GEISER, E.A.: Speckle Reduction and Contrast Enhancement of Echocardiograms via Multiscale Nonlinear Processing, IEEE Transaction on Medical Imaging **17** No. 4 (1998), 532–540.

[8] GEHLBACH, S.M.—SOMMER, G.F.: Speckle Reduction Processing, Internat. Sympos. on Pattern Recogn. and Acoustical Imaging, 1987.

[9] STETSON, P.F.—SOMMER, F.G.—MACKOVSKI, A.: Lesion Contrast Enhancement in Medical Ultrasound Imaging, IEEE Transaction on Medical Imaging **16** No. 4 (1997), 416–425.

[10] STRANG, G.—NGUYEN, T.: Wavelets and Filter Banks, Wellesley, Wellesley-Cambridge Press, 1996.

Received 22 November 2002

Radim Kolář was born in 1975. Education and academic degrees: BSc in Electrical Engineering, Brno University of Technology in 1997, MSc in Automatic Control and Measurement in combination with Biomedical Engineering from the Brno University of Technology in 1998, PhD in Biomedical Engineering (Methods for preprocessing of medical ultrasound tomograms) in 2002. Teaching activities: signal processing, programming. Scientific activities: image and signal analysis and restoration, including biomedical applications, ultrasound imaging, 3D imaging

Jiří Kozumplík was born in 1949. Education and academic degrees: MSc in Electrical Engineering (Brno Technical University of Technology, 1973), PhD in Biomedical Engineering (Brno Technical University of Technology, 1992). Teaching activities: Signals and systems, advanced signal processing, fuzzy expert systems. Research activities: Digital signal processing, processing and analysis of biosignals, data compression, wavelet transform application, fuzzy systems, ultrasound processing.